Acta Oceanol. Sin., 2024, Vol. 43, No. 10, P. 33–39
https://doi.org/10.1007/s13131-024-2378-8
http://www.aosocean.com
E-mail: ocean2@hyxb.org.cn

Observed features of stable surface seawater isotopes across the Pacific, Indian and Southern oceans

Xuemei Wu[1, 2], Weijun Sun[1], Biao Tian[2], Baojuan Huai[1], Zhiheng Du[3], Minghu Ding[2*]

[1] College of Geography and Environment, Shandong Normal University, Jinan 250014, China

[2] State Key Laboratory of Severe Weather, Chinese Academy of Meteorological Sciences, Beijing 100081, China

[3] State Key Laboratory of Cryospheric Science, Northwest Institute of Eco-Environment and Resources, Chinese Academy of Sciences, Lanzhou 730000, China

Received 29 January 2024; accepted 24 March 2024

Abstract

The marine hydrological process is still unclear due to scarce observations. Based on stable water isotopes in surface seawater along the 33rd Chinese National Antarctic Science Expedition from November 2016 to April 2017, this study explored the hydrological processes in the Pacific, Indian and Southern oceans. The results show that the Northwest Pacific (0°–26°N) is a region with strong evaporation (the δ^{18}O-δD slope is 6.58), while the southern Indian Ocean is a region with strong precipitation (the δ^{18}O-δD slope is 9.57). The influence of continental runoff and water mass mixing reduces the correlation between δ^{18}O and salinity in the eastern Indian Ocean. The characteristics of the isotopes and hydrological parameters indicate that the Agulhas Front and sub-Tropical Convergence do not merge in the Antarctic–Indian Ocean region. The freezing of sea ice near the Antarctic continent decreases the δ^{18}O and δD by 0.40‰ and 7.0‰, respectively, compared with those near 67°S. This study is helpful for understanding marine hydrological processes and promoting the understanding and research of the nature of ocean responses in the context of climate change.

Key words: spatial variability, surface seawater isotopes, δ^{18}O-salinity relation, water mass fronts

Citation: Wu Xuemei, Sun Weijun, Tian Biao, Huai Baojuan, Du Zhiheng, Ding Minghu. 2024. Observed features of stable surface seawater isotopes across the Pacific, Indian and Southern oceans. Acta Oceanologica Sinica, 43(10): 33–39, doi: 10.1007/s13131-024-2378-8

1 Introduction

Isotopic composition, expressed as δ^{18}O and δD relative to the Vienna Standard Mean Ocean Water (V-SMOW) of seawater, represents the ratio of light and heavy water molecules (Coplen, 1994; Masson-Delmotte et al., 2003). Hydrogen and oxygen isotopes, akin to salinity, are widely utilized in hydrology and contemporary oceanography for tracking hydrological processes such as evaporation/precipitation, continental runoff, and sea ice freeze-thaw (Kiran Kumar et al., 2018; Lao et al., 2023b; Lao et al., 2022a; Reyes-Macaya et al., 2022; Frew et al., 1995; Khim et al., 1997; Srivastava et al., 2007; Xu et al., 2012). However, compared to traditional methods like the temperature-salinity relationship, satellite remote sensing and numerical simulation for studying hydrological processes, water isotopes offer inherent advantages and can serve as tracers for water (Lao et al., 2022b; Lao et al., 2023a). Furthermore, isotopes find extensive application in paleoclimate reconstruction, and the combination of δ^{18}O and δD can mitigate error of paleosalinity reconstruction (Sowers and Bender, 1995; LeGrande and Schmidt, 2011).

Research indicates that while water isotopes and salinity lack direct mechanistic connections, they exhibit an empirical relationship profoundly influenced by hydrological processes (Deshpande et al., 2013; Belem et al., 2019; Lao et al., 2023a). Numerous factors, including continental runoff, evaporation/precipitation, water mass mixing and sea ice freezing/melting, can influence the δ^{18}O-salinity relationship (Singh et al., 2010). During evaporation and precipitation, salinity and δ^{18}O exhibit proportional changes, whereas hydrological processes like water mass mixing and continental runoff may influence the δ^{18}O-salinity through salinity (Sengupta et al., 2013; Kiran Kumar et al., 2018; Reyes-Macaya et al., 2022; Lao et al., 2023a). Consequently, the integration of water isotopes and hydrological parameters can delineate the linear relationship between local surface seawater δ^{18}O and salinity, thereby characterizing the hydrological and climatic features of the region (Srivastava et al., 2007).

The isotopic values of water masses are influenced not only by circulation but also by processes such as evaporation/precipitation and melting/freezing (Wu et al., 2021; Benetti et al., 2017; Lao et al., 2022b; Reyes-Macaya et al., 2022). Studies have shown that oceans from the tropics to the Antarctic continent exhibit pronounced latitudinal zoning, with physical factors such as evaporation/precipitation and melting/freezing having varying effects (Rahul et al., 2018). Freshwater sources (such as precipitation and river transport), evaporation processes, changes in ocean currents, and vertical mixing of water masses contribute to alterations in Pacific seawater salinity, oxygen isotopes and their relationships (Conroy et al., 2014). The isotopic composition of seawater also reflects the characteristics of surface seawater in various frontal systems in the Southern Ocean and Indian Ocean (Tiwari et al., 2013). The Southern Ocean, surrounding Antarc-

Foundation item: The National Natural Science Foundation of China under contract No. 42122047; the Basic Research Fund of Chinese Academy of Meteorological Sciences under contract Nos 2021Z006, 2023Z015 and 2023Z005; the Chinese National Antarctic Science Expedition.

*Corresponding author, E-mail: dingminghu@foxmail.com

tica, possesses a unique marine dynamic environment and serves as the source of the majority of the middle and bottom waters of the world's oceans (Archambeau et al., 1998). Additionally, the Southern Ocean plays a pivotal role in climate change (Chen et al., 2023). It is characterized by several narrow ocean fronts exhibiting substantial variability in salinity, temperature, and nutrients (Lutjeharms and Valentine, 1984; Belkin and Gordon, 1996). Research has identified two prominate sea water fronts in the Indian Ocean and Southern Ocean: the Agulhas Front and Sub-Tropical Convergence (Rintoul and England, 2002). However, previous studies predominantly relied on temperature and salinity data to delineate the existence of fronts. Alternatively, stable isotopes, salinity, and temperature can all serve as indicators of the presence of an ocean front (Srivastava et al., 2007). Although hydrological processes in the Pacific, Indian and Southern oceans have been studied, understanding of these processes in these area remains incomplete due to data limitations (e.g., hydrogen & oxygen isotope date bases, GISS & GNIP data bases) (LeGrande and Schmidt, 2006; Srivastava et al., 2007; Kiran Kumar et al., 2018).

This paper present a spatial analysis conducted on isotopic and salinity data obtained from surface seawater collected during the 33rd Chinese National Antarctic Science Expedition (CHINARE) spanning from East China Sea to Pritz Bay, Antarctica, conducted from November 2016 to April 2017.

2 Data and methods

The 33rd CHINARE commenced from Shanghai in November 2016, traversing the East China Sea, Pacific Ocean, Indonesian waters, Indian Ocean and Southern Ocean before reaching Pritz Bay, Antarctica. It concluded in April 2017 upon its return to Shanghai, during which seawater samples were collected en route. The sampling points are delineated in Fig. 1. Samples were collected using 250 mL high-density polyethylene (HDPE) narrow mouth bottles to minimize liquid evaporation. A total of fifty-nine surface seawater samples were acquired throughout the expedition's return journey. Each sample bottle was subsequently sealed within an individual plastic bag and stored in a refrigerator at a temperatures ranging from 3℃ to 5℃.

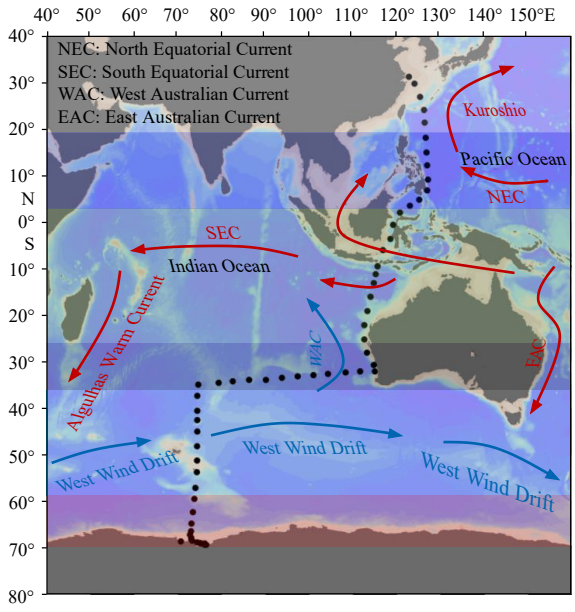

Fig. 1. Isotope sampling sites in surface seawater of the 33rd CHINARE.

The isotopic composition of stable seawater was analyzed using wavelength scanning cavity ring-down spectroscopy (CRDS) with a Picarro L1102 instrument at the Chinese Academy of Meteorological Science. The total accuracy of $\delta^{18}O$ is better than 0.15‰, and δD is better than 0.5‰. The Picarro analyzer utilizes a time-based, optical absorption spectrum of the target gas to determine element concentrations. It has demonstrated reliability in stable water isotope analysis and has been widely utilized (Tian et al., 2018; Skrzypek and Ford, 2014).

Owing to the influence of hydrological processes such as water mass mixing and ocean circulation, the composition of isotopes in the local ocean undergoes rapid changes (Ren and Wang, 2000). To delineate the spatial distribution of stable surface seawater isotopes and salinity more comprehensively, we utilized data from the return journey for clustering and employed a clustering model for quantitative analysis. The relationship between $\delta^{18}O$ and δD can be expressed as follow:

$$\delta D = S \times \delta^{18}O + d, \tag{1}$$

where S represents the coefficient, while d denotes a constant term. S and d are expected to exhibit similarity in areas with the same humidity source. Researchers have identified a robust linear relationship between S and d in their investigation of stable seawater isotopes (Kang et al., 2009):

$$d = aS + k, \tag{2}$$

where a represents the coefficient, while k signifies a constant term. In this equation, the disparity between a and k signifies differences in water sources. In mathematics, r^2 (correlation index) serves as an indicator of the reliability of estimation in a unary polynomial regression equation. Consequently, we computed the r^2 of $d = aS + k$ for sampling points along the journey line.

$$r^2 = 1 - \frac{\sum_{i=1}^{n} (d_i - \widehat{d}_i)^2}{\sum_{i=1}^{n} (d_i - \bar{d})^2}. \tag{3}$$

The correlation indices of (S_1, d_1), (S_2, d_2), (S_3, d_3), ⋯, (S_n, d_n) are denoted as r_a^2, while the correlation index of the remaining arrays is denoted as r_b^2. The optimal breakpoints of clustering are determined using r_a^2 and r_b^2. A higher r^2 value indicates a better fitting effect of the model. Therefore, when the $r_a^2 + r_b^2$ reaches its maximum value, it indicates the optimal breakpoint. One-way analysis of variance was employed to test the statistical difference between groups at a significant level of 0.05 (Li et al., 2022).

3 Results

3.1 *Spatial distribution of $\delta^{18}O$, δD and salinity*

Through the aforementioned analysis, five clusters were identified and depicted in Fig. 2. Cluster 1 is situated near the Antarctic continent, spanning latitudes between 59°S and 70°S. Within this range, both sea surface temperature (SST) and δ exhibit a gradual decrease with latitude, while salinity remains relatively constant. The decline in $\delta^{18}O$ and δD in precipitation is attributed to sea ice and glacial melt water as latitude increases (Tiwari et al., 2013). However, the excess deuterium (d) value in this region suggests minimal variations in evaporation, resulting in

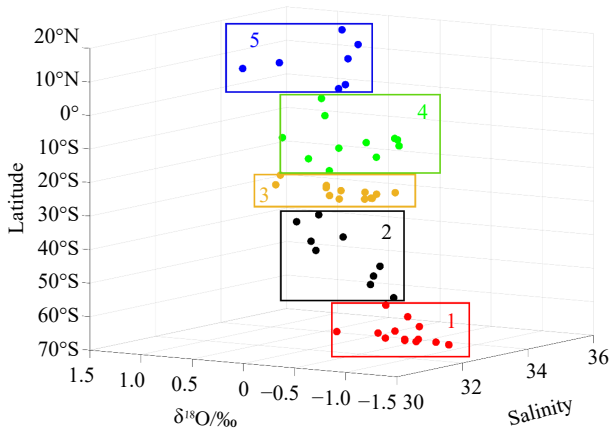

Fig. 2. Three-dimensional plot showing $\delta^{18}O$, salinity, latitude.

slight changes in salinity. Near Antarctica, the freezing and melting processes of sea ice cause significant fluctuations in stable surface seawater isotopes. Cluster 2 is positioned in the Indian Ocean region of the Southern Ocean, where $\delta^{18}O$, δD and salinity increase with latitude. This pattern is consistent with similar latitudinal trends observed in the Pacific and Atlantic regions (LeGrande and Schmidt, 2006). Cluster 3 is situated on the southern side of the Indian Ocean and the southwestern side of Australia, spanning latitudes between 28°S and 35°S. Due to the narrow latitude span, SST and salinity exhibit minimal variation in Cluster 3. This area is characterized by high SST and salinity, serving as an enrichment area of $\delta^{18}O$ and δD. Cluster 4 is located in Indonesian waters and the western side of Australia, with latitudes between 2°N and 26°S. Cluster 4 experiences high SST, leading to $\delta^{18}O$, δD and salinity predominantly influenced by evaporation and precipitation. Cluster 5 predominantly resides in the Pacific Ocean, spanning latitudes between 3°N and 20°N, primarily affected by the North Equatorial Current.

The $\delta^{18}O$ values of surface seawater range from −1.39‰ to 1.49‰, and decreases noticeably with latitude (Fig. 3). Enriched values are observed in middle and low latitudes, while depleted values are found in high latitudes. Near 30°N, both $\delta^{18}O$ and δD exhibit abnormally low values of −1.39‰ and −5.3‰, respectively, due to the influence of freshwater flushing near the

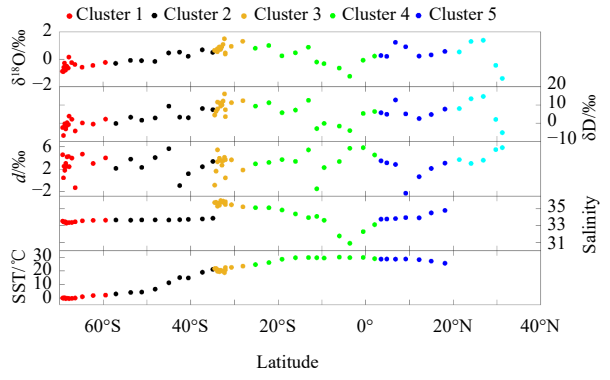

Fig. 3. Spatial variations of $\delta^{18}O$, δD, excess deuterium (d), salinity and SST (due to the absence of salinity and SST data for samples between 20°N and 35°N, data from 70°S to 20°N are clustered together). Different colored points represent various clusters, ranging from 70°S to 20°N, labeled as Cluster 1, Cluster 2, Cluster 3, Cluster 4. and Cluster 5 (n = 54).

Changjiang River. Between 20°N and 10°N, $\delta^{18}O$ and δD values decrease continuously, accompanied by a decrease in salinity by 0.53 following the $\delta^{18}O$ pattern, indicative of increased precipitation. From 10°N to 5°N, $\delta^{18}O$, δD and salinity values increased by 1.02‰, 7.9‰ and 0.05, respectively, reflecting the evaporation effect in this region (Srivastava et al., 2007). At 3.6°S, a low salinity and low oxygen zone emerges, influenced by the Inter Tropical Convergence Zone as a rainfall area. From 5°S to 30°S, salinity continues to increase alongside $\delta^{18}O$ and δD, albeit with some minor fluctuations. South of 30°S, $\delta^{18}O$ enrichment is observed in seawater with high salinity, indicative of a high evaporation area (Rahul et al., 2018). From 32.3°S to 62°S, both $\delta^{18}O$ and δD continue to decline due to the gradual change of ocean surface environment from warm to cold. Notably, a transition zone exsits between the Agulhas Front and the Sub-Tropical Convergence near 42°–44°S, leading to significant changes in isotopic composition and SST in the region (Srivastava et al., 2007), which will be discussed in detail in Discussion Section. From 65°S to 67.8°S, salinity decreased by 0.20, while $\delta^{18}O$ and δD increased by 0.74‰ and 3.7‰, respectively, due to the melting of sea ice. South of 67.8°S, both $\delta^{18}O$ and δD decrease to −0.91‰ and −6.9‰, respectively, and salinity increases to 33.43, reflecting the phenomenon of sea ice freezing in this region. Salinity of ocean water is much higher than that of sea ice. The melting of sea ice reduces the salinity of surface water, whereas salt rejection occurs during sea ice freezing, thereby increasing the salinity of surface water (Rohling, 2013). Additionally, molecular fractionation occurs during the freezing and melting of sea ice, which heavier molecules (^{18}O and ^{2}H) being preferentially incorporated into the sea ice (Brennan et al., 2013).

3.2 *δD and δ18O relationship*

The observational results demonstrate a robust correlation between δD and $\delta^{18}O$ in the surface waters spanning from the Pacific Ocean to the Southern Ocean (r = 0.89, P < 0.001), with a slope of δD-$\delta^{18}O$ is 7.67, closely resembling the global average δD-$\delta^{18}O$ slope of 7.4 (Rohling, 2007). Additionally, through clustering analysis, we observed a significantly correlation between δD and $\delta^{18}O$ in the surface seawater across different sea areas (Fig. 4). Cluster 5 exhibits the lowest slope of 6.58, indicating extremely strong evaporation in this region. Given the subsolar point's proximity to the northern equator in April, evaporation

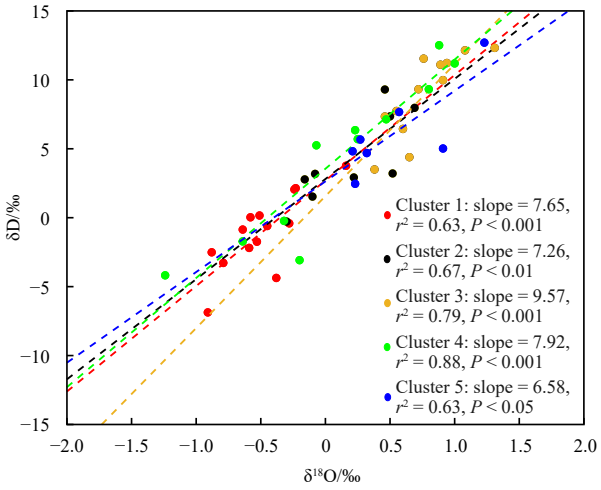

Fig. 4. The relationship between δD and $\delta^{18}O$ in surface seawater.

intensifies within Cluster 5. Cluster 1 and Cluster 2 exhibits slopes of δD and $\delta^{18}O$ at 7.65 and 7.26, respectively, closely resembling the global average seawater slope of 7.4 (Rohling, 2007). The slope of Cluster 2 remains lower than the global average δD-$\delta^{18}O$ slope, suggesting continued influence by evaporation in this region. The slope of Cluster 1 is marginally higher than the global average seawater slope. With the slope of 7.92, Cluster 4 surpasses the global average seawater slope, indicating precipitation dominance in this region. Furthermore, this is corroborated by the slope of the global rainfall line (8.0), closely resembling the slope of global rainfall (Chen et al., 2021; Lao et al., 2022b). Cluster 3 exhibits the highest slope of δD and $\delta^{18}O$ at 9.57 in the southern Indian Ocean indicating strong precipitation influence. The region is influenced by westerly winds and experiences higher precipitation, resulting in a generally higher slope. This suggests that a significant role of local precipitation and evaporation in the δD-$\delta^{18}O$ relationship.

4 Discussion

Factor such as evaporation/precipitation, freezing/melting of sea ice, advection and diffusion of water masses impact the stable seawater isotopic composition (Lao et al., 2023b, 2022a, 2022b). Figure 5 illustrates a stable positive correlation between $\delta^{18}O$-salinity and δD-salinity along the entire route, with slopes of 0.437‰ per practical salinity unit for $\delta^{18}O$ ($n = 54$, $P < 0.001$) and 3.213‰ per practical salinity unit for δD ($n = 54$, $P < 0.001$). Given that precipitation and evaporation influence salinity and δ concurrently, the linear correlation between salinity and $\delta^{18}O$ (or δD) (Fig. 5) implies that stable isotopes in surface seawater are predominantly influenced by evaporation and precipitation. In order to further study the specific isotopic variability across different sea areas, the relationship between salinity and $\delta^{18}O$ in distinct seas was delineated through data clustering (Fig. 6). Cluster 2 exhibits a substantial slope of 3.07 ‰ per practical salinity unit ($r^2 = 0.41$, $P < 0.10$), suggesting that additional hydrological processes besides evaporation/precipitation important to $\delta^{18}O$ and salinity values in this region. Cluster 4 exhibits a slope of 0.41‰ per practical salinity unit ($r^2 = 0.71$, $P < 0.01$), suggesting these regions may primarily be influenced by precipitation/evaporation. The slopes of Cluster 1, Cluster 3 and Cluster 5 were −0.14‰ per practical salinity unit, −0.38‰ per practical salinity unit and −0.06‰ per practical salinity unit, respectively, however, the effect was not statistically significant ($r^2 < 0.1$, $P > 0.1$). Cluster 1 is situated near the Antarctic continent, where the salinity of the surface water influenced by sea ice , remains relatively stable. Cluster 3 is situated in the Indian Ocean region, affected by the Indian Ocean tropical front, the Indian-Pacific warm pool, and the Indian and Pacific monsoon and the Australian mainland also have a notable impact on the salinity of the Indian Ocean (Ummenhofer et al., 2021). The insignificance of cluster 5 may be attributed to the sampling sites near 10°N, which are in proximity to Southeast Asia, where surface runoff carries a substantial amount freshwater (Yu and McCreary, 2004).

Evaporation, freshwater input from the Changjiang River and water mass mixing processes are notable in the Northwest Pacific (10°S–32°N). The influx of water from the Changjiang River near 30°N leads to decrease in $\delta^{18}O$ and δD in surface seawater near the continent (Figs 1 and 3). The Pacific region near 10°N experiences significant evaporation, resulting in high value of $\delta^{18}O$ and salinity (Figs 3 and 4). In the vicinity of Southeast Asia, the Pacific Ocean experiences not only freshwater input but also the mixing of various water masses. Previous studies have also confirmed the presence of water mass mixing in the Northwest Pacific (Kiran Kumar et al., 2018; Chen et al., 2021).

The mixing process of water masses, sea ice and freeing/melting of continental ice shelves are noteworthy in the Indian Ocean region (north of 60°S) and the Southern Ocean (south of 60°S). Figure 7b illustrates the position and SST of the water mass front. The Agulhas Front observed in this study is positioned between 37°S and 41°S , as determined by the SST range of the front (15.7–21℃) (Srivastava et al., 2007). Likewise, the pronounced decrease in $\delta^{18}O$, δD, SST and salinity also corroborates the existence of the Agulhas Front at this position (Fig. 3). Lutjeharms demonstrated that the Agulhas Front was situated between 39°09′S and 40°01′S, with an intermediate position at 39°37′S (Lutjeharms and Valentine, 1984). While the position of the Agulhas Front we observed closely aligns with that observed by Lutjeharm, it is slightly displaced northward. The Sub-Tropical Convergence intersecting the southern edge of the Agulhas Front exhibited the SST drop of 4.2℃. The decrease in SST we observed may be attributed to the lack of a combined state between the Agulhas Front and Sub-Tropical Convergence, as their combination typically results in an increase in average SST. This phenomenon difference with the observation of the merging of the Agulhas Front and Sub-Tropical Convergence in the Southern Ocean of southern Africa (Lutjeharms and Valentine, 1984). Between 45°S and 48°S, there is a $\delta^{18}O$ variation of 0.62‰, indicating the presence of Sub-Antarctic Front, which corresponds to

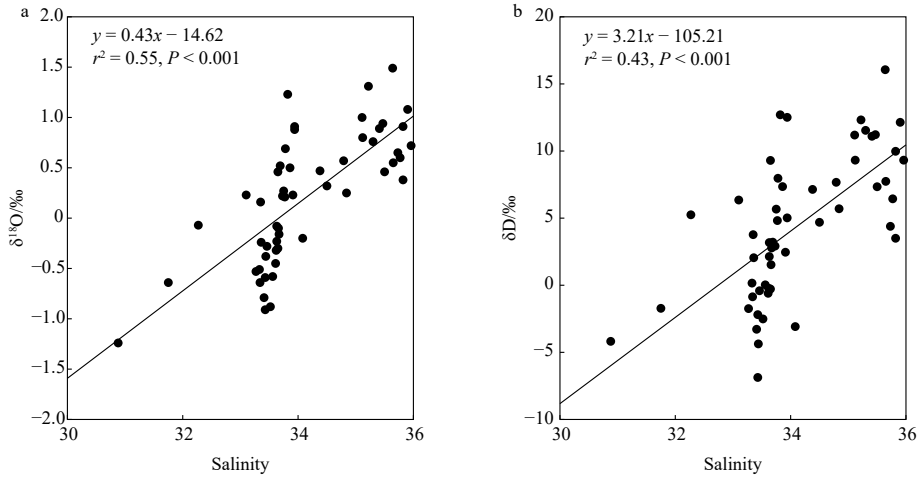

Fig. 5. The quantitative relationship between $\delta^{18}O$, δD and salinity.

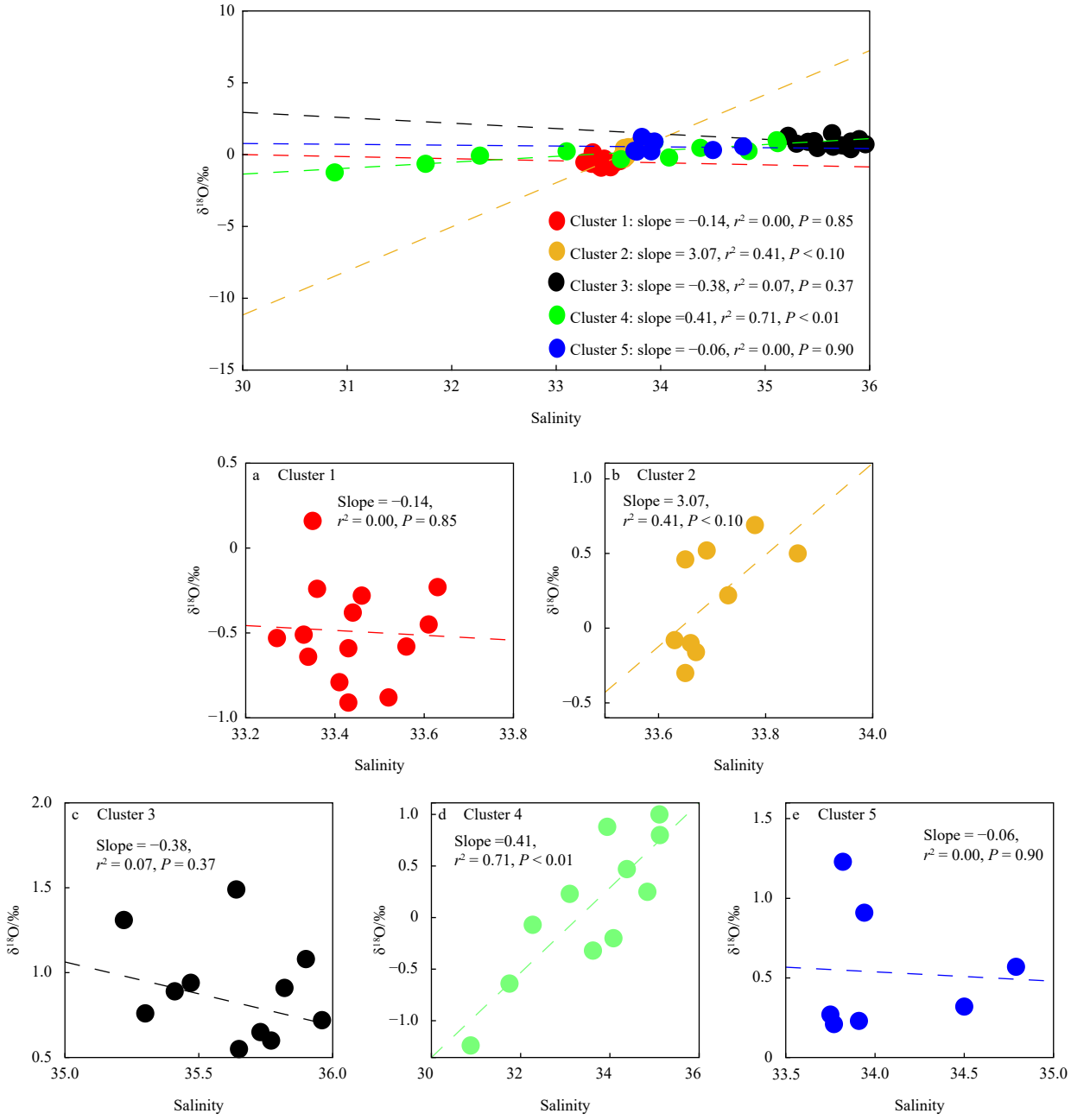

Fig. 6. The relationship between salinity and $\delta^{18}O$ in different sea areas.

the most notable drop in SST in this region (Figs 3 and 7b). The Antarctic Polar Front is located at 52°–62°S with the SST range of 4.0–1.8℃. Figure 7a illustrates significant variability in the salinity of surface seawater near the Antarctic continent, suggesting the influence of sea ice freezing/melting, in conjunction with the isotopic changes discussed in Section 3.1. The SST fluctuates around 0℃ due to the heat absorption and release from melting and freezing sea ice. In summary, our findings indicate that in the Indian Ocean and the Southern Ocean, the Agulhas Front exists independently and does not merge with the Sub-Tropical Convergence. Additionally, the Agulhas Front exhibits a slight northward shifted.

5 Conclusions

In this study, we conducted new measurements of hydrogen and oxygen stable isotopes in surface seawater along the route of the 33rd CHINARE, thereby expanding the global surface seawater isotope dataset. By analyzing isotope composition, the relationship between $\delta^{18}O$ and δD, the relationship between $\delta^{18}O$ and salinity, and SST using this new dataset, we aimed to track hydrological processes and assess the impacts of water mass fronts.

This study revealed that the stable isotopic composition of surface seawater has obvious latitudinal distribution characteristics and that $\delta^{18}O$ and δD decrease with increasing latitude. Due to the effects of evaporation/precipitation, there is a strong correlation between $\delta^{18}O$ and δD in different sea areas. The area north of the equator is affected by strong evaporation, and the slope of $\delta^{18}O$-δD is 6.58, which is significantly lower than the global average seawater slope. Strong precipitation causes the $\delta^{18}O$-δD slope to reach 9.57 in the southern Indian Ocean. The

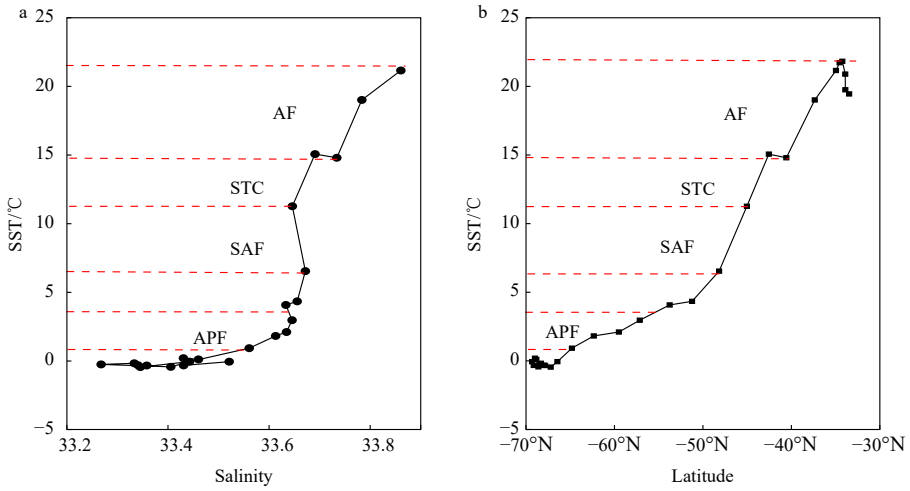

Fig. 7. The change of temperature field. a. The relationship between SST and salinity, b. the relationship between surface sea temperature and latitude. AF: Agulhas Front; STC: Sub-Tropical Convergence; SAF: Sub-Antarctic Front; APF: Antarctic Polar Front.

$\delta^{18}O$, δD, SST and salinity indicate that the Agulhas Front is located at 35°–41°S and that the Agulhas Front and Sub-Tropical Convergence do not merge in the Indian Ocean region of the Southern Ocean. The existence of water mass fronts has a great influence on the $\delta^{18}O$-salinity relationship in this area. The freezing of sea ice near the Antarctic continent has led to a significant increase in surface seawater salinity and a decrease in $\delta^{18}O$ and δD.

This study can help us understand the spatial variation in stable seawater isotopes along the route from the Pacific to Southern Ocean, establish stable $\delta^{18}O$-δD relationships, and further understand the hydrological processes in the Pacific Ocean, Indian Ocean, and Southern Ocean. Due to the different sampling seasons, isotope variation may also show differences. However, to further study the spatial differences in stable surface seawater isotopes at different times, a longer sampling time is needed, which is the direction of our subsequent research.

References

Archambeau A S, Pierre C, Poisson A, et al. 1998. Distributions of oxygen and carbon stable isotopes and CFC-12 in the water masses of the Southern Ocean at 30°E from South Africa to Antarctica: results of the CIVA1 cruise. Journal of Marine Systems, 17(1–4): 25–38, doi: 10.1016/S0924-7963(98)00027-X

Belem A L, Caricchio C, Albuquerque A L S, et al. 2019. Salinity and stable oxygen isotope relationship in the Southwestern Atlantic: constraints to paleoclimate reconstructions. An Acad Bras Cienc, 91(3): e20180226, doi: 10.1590/0001-3765201920180226

Belkin I M, Gordon A L. 1996. Southern Ocean fronts from the Greenwich meridian to Tasmania. Journal of Geophysical Research: Oceans, 101(C2): 3675–3696, doi: 10.1029/95JC02750

Benetti M, Reverdin G, Aloisi G, et al. 2017. Stable isotopes in surface waters of the Atlantic Ocean: Indicators of ocean-atmosphere water fluxes and oceanic mixing processes. Journal of Geophysical Research: Oceans, 122(6): 4723–4742, doi: 10.1002/2017JC012712

Brennan C E, Meissner K J, Eby M, et al. 2013. Impact of sea ice variability on the oxygen isotope content of seawater under glacial and interglacial conditions. Paleoceanography, 28(3): 388–400, doi: 10.1002/palo.20036

Chen Fajin, Huang Chao, Lao Qibin, et al. 2021. Typhoon control of precipitation dual isotopes in Southern China and its palaeoenvironmental implications. Journal of Geophysical Research: Atmospheres, 126(14): e2020JD034336, doi: 10.1029/2020JD034336

Chen Yangjun, Chen Jinxu, Wang Yi, et al. 2023. Sources and transformations of nitrite in the Amundsen Sea in summer 2019 and 2020 as revealed by nitrogen and oxygen isotopes. Acta Oceanologica Sinica, 42(4): 16–24, doi: 10.1007/s13131-022-2111-4

Conroy J L, Cobb K M, Lynch-Stieglitz J, et al. 2014. Constraints on the salinity–oxygen isotope relationship in the central tropical Pacific Ocean. Marine Chemistry, 161: 26–33, doi: 10.1016/j.marchem.2014.02.001

Coplen T B. 1994. Reporting of stable hydrogen, carbon, and oxygen isotopic abundances (Technical Report). Pure and Applied Chemistry, 66(2): 273–276, doi: 10.1351/pac199466020273

Deshpande R D, Muraleedharan P M, Singh R L, et al. 2013. Spatio-temporal distributions of $\delta^{18}O$, δD and salinity in the Arabian Sea: Identifying processes and controls. Marine Chemistry, 157: 144–161, doi: 10.1016/j.marchem.2013.10.001

Frew R D, Heywood K J, Dennis P F. 1995. Oxygen isotope study of water masses in the Princess Elizabeth Trough, Antarctica. Marine Chemistry, 49(2–3): 141–153, doi: 10.1016/0304-4203(95)00003-A

Kang Jiancheng, Jouzel J, Stievenard M, et al. 2009. Variation of stable isotopes in surface snow along a traverse from coast to plateau's interior in East Antarctica and its climatic significance. Sciences in Cold and Arid Regions, 1(1): 14–24

Khim B K, Park B K, Yoon H I. 1997. Oxygen isotopic compositions of seawater in the Maxwell Bay of King George Island, West Antarctica. Geosciences Journal, 1(2): 115–121, doi: 10.1007/BF02910483

Kiran Kumar P, Singh A, Ramesh R. 2018. Controls on $\delta^{18}O$, δD and $\delta^{18}O$-salinity relationship in the northern Indian Ocean. Marine Chemistry, 207: 55–62, doi: 10.1016/j.marchem.2018.10.010

Lao Qibin, Lu Xuan, Chen Fajin, et al. 2023a. A comparative study on source of water masses and nutrient supply in Zhanjiang Bay during the normal summer, rainstorm, and typhoon periods: insights from dual water isotopes. Science of the Total Environment, 903: 166853, doi: 10.1016/j.scitotenv.2023.166853

Lao Qibin, Lu Xuan, Chen Fajin, et al. 2023b. Effects of upwelling and runoff on water mass mixing and nutrient supply induced by typhoons: Insight from dual water isotopes tracing. Limnology and Oceanography, 68(1): 284–295, doi: 10.1002/lno.12266

Lao Qibin, Wu Junhui, Chen Fajin, et al. 2022a. Increasing intrusion of high salinity water alters the mariculture activities in Zhanjiang Bay during the past two decades identified by dual water isotopes. Journal of Environmental Management, 320: 115815, doi: 10.1016/j.jenvman.2022.115815

Lao Qibin, Zhang Shuwen, Li Zhiyang, et al. 2022b. Quantification of the seasonal intrusion of water masses and their impact on nutrients in the Beibu Gulf using dual water isotopes. Journal of Geophysical Research: Oceans, 127(7): e2021JC018065, doi: 10.

1029/2021JC018065
LeGrande A N, Schmidt G A. 2006. Global gridded data set of the oxygen isotopic composition in seawater. Geophysical Research Letters, 33(12): L12604
LeGrande A N, Schmidt G A. 2011. Water isotopologues as a quantitative paleosalinity proxy. Paleoceanography, 26(2): PA3225
Li Zhiqiang, Ding Minghu, Wang Yetang, et al. 2022. Spatial variability of $\delta^{18}O$ and $\delta^{2}H$ in North Pacific and Arctic Oceans surface seawater. Advances in Polar Science, 33(3): 244–252
Lutjeharms J R E, Valentine H R. 1984. Southern ocean thermal fronts south of Africa. Deep-Sea Research Part A: Oceanographic Research Papers, 31(12): 1461–1475
Masson-Delmotte V, Delmotte M, Morgan V, et al. 2003. Recent southern Indian Ocean climate variability inferred from a Law Dome ice core: new insights for the interpretation of coastal Antarctic isotopic records. Climate Dynamics, 21(2): 153–166, doi: 10.1007/s00382-003-0321-9
Rahul P, Prasanna K, Ghosh P, et al. 2018. Stable isotopes in water vapor and rainwater over Indian sector of Southern Ocean and estimation of fraction of recycled moisture. Scientific Reports, 8(1): 7552, doi: 10.1038/s41598-018-25522-5
Ren Jianguo, Wang Xianbin. 2001. Helium and Oxygen isotopic evidence on the exchange of water between the West Pacific and the South China Sea. Haiyang Xuebao (in Chinese), 23(2): 57–61
Reyes-Macaya D, Hoogakker B, Martínez-Méndez G, et al. 2022. Isotopic characterization of water masses in the Southeast Pacific region: paleoceanographic implications. Journal of Geophysical Research: Oceans, 127(1): e2021JC017525, doi: 10.1029/2021JC017525
Rintoul S R, England M H. 2002. Ekman transport dominates local air-sea fluxes in driving variability of subantarctic mode water. Journal of Physical Oceanography, 32(5): 1308–1321, doi: 10.1175/1520-0485(2002)032<1308:ETDLAS>2.0.CO;2
Rohling E J. 2007. Progress in paleosalinity: Overview and presentation of a new approach. Paleoceanography, 22(3): PA3215
Rohling E J. 2013. Oxygen isotope composition of seawater. In: Elias S A, ed. Encyclopedia of Quaternary Science. Amsterdam: Elsevier, 915–922
Sengupta S, Parekh A, Chakraborty S, et al. 2013. Vertical variation of oxygen isotope in Bay of Bengal and its relationships with water masses. Journal of Geophysical Research: Oceans, 118(12): 6411–6424, doi: 10.1002/2013JC008973
Singh A, Jani R A, Ramesh R. 2010. Spatiotemporal variations of the $\delta^{18}O$-salinity relation in the northern Indian Ocean. Deep-Sea Research Part I: Oceanographic Research Papers, 57(11): 1422–1431, doi: 10.1016/j.dsr.2010.08.002
Skrzypek G, Ford D. 2014. Stable isotope analysis of saline water samples on a cavity ring-down spectroscopy instrument. Environmental Science & Technology, 48(5): 2827–2834
Sowers T, Bender M. 1995. Climate records covering the last deglaciation. Science, 269(5221): 210–214, doi: 10.1126/science.269.5221.210
Srivastava R, Ramesh R, Prakash S, et al. 2007. Oxygen isotope and salinity variations in the Indian sector of the Southern Ocean. Geophysical Research Letters, 34(24): L24603
Tian Biao, Sun Weijun, Ding Minghu, et al. 2018. Analytical method and performance research for determination of hydrogen and oxygen stable isotopes ratio in water sample by using new type of laser spectrum analyzer. China Measurement & Test, 44(2): 122–127
Tiwari M, Nagoji S S, Kartik T, et al. 2013. Oxygen isotope-salinity relationships of discrete oceanic regions from India to Antarctica vis-à-vis surface hydrological processes. Journal of Marine Systems, 113–114: 88–93
Ummenhofer C C, Murty S A, Sprintall J, et al. 2021. Heat and freshwater changes in the Indian Ocean region. Nature Reviews Earth & Environment, 2(8): 525–541
Wu Junhui, Lao Qibin, Chen Fajin, et al. 2021. Water mass processes between the South China Sea and the Western Pacific through the luzon strait: insights from hydrogen and oxygen isotopes. Journal of Geophysical Research: Oceans, 126(8): e2021JC017484, doi: 10.1029/2021JC017484
Xu Xu, Werner M, Butzin M, et al. 2012. Water isotope variations in the global ocean model MPI-OM. Geoscientific Model Development, 5(3): 809–818, doi: 10.5194/gmd-5-809-2012
Yu Zhiyu, McCreary Jr J P. 2004. Assessing precipitation products in the Indian Ocean using an ocean model. Journal of Geophysical Research: Oceans, 109(C5): C05013